Mass Spectrometry Imaging of Lipids In A Gut Epithelial Cell Model

Hadeer Mattar
The University of Manchester Manchester Institute of Biotechnology
Emmanuelle Claude
Waters Corp
Lee Gethings
Waters Corp
Clare Mills (clare.mills@manchester.ac.uk)
The University of Manchester https://orcid.org/0000-0001-7433-1740

Research Article

Keywords: Gut epithelium, Caco2, HT29-MTX, mass spectrometry imaging, lipids.

Posted Date: February 28th, 2022

DOI: https://doi.org/10.21203/rs.3.rs-1108246/v1

Mass Spectrometry Imaging of Lipids in a Gut Epithelial Cell Model

Hadeer Mattar[1] (Orcid ID: 0000-0001-6123-9443), Emmanuelle Claude[2], Lee Gethings[2], E. N. Clare Mills[1] (Orcid ID 0000-0001-7433-1740)

[1]Division of Infection, Immunity and Respiratory Medicine, Manchester Academic Health Sciences Centre, Manchester Institute of Biotechnology, University of Manchester, Manchester, M1 7DN, UK.

[2]Water Corporation, Stamford Avenue, Altrincham Road, Wilmslow, SK9 4AX, UK.

Correspondence: Professor Clare Mills, clare.mills@manchester.ac.uk

Keywords:

Gut epithelium, Caco2, HT29-MTX, mass spectrometry imaging, lipids.

Abstract

Scope: The Caco2/HT29-MTX co-culture system is widely used as a cell model of the intestinal epithelium. Although the gut epithelium plays an important role in the uptake of free fatty acids and the resynthesis of triglycerides the lipid distribution profile of the co-culture system is not well understood. Desorption electrospray ionization (DESI) is a mass spectrometry (MS) technique which has been widely used to study the main classes of lipid molecules on different tissue surfaces. This has been used to map lipid species and their distribution in Caco2 and HT29-MTX co-culture system.

Methods and results: Caco2 and HT29-MTX cells were seeded on coverslips either singly or as cocultures in ratios of 75:25 and 50:50. Cells were cultured for 21 days before MS imaging using a DESI source in both the positive and negative ionization modes. The identity of selected lipids was confirmed in negative and positive ionisation modes using tandem MS. Although many lipids were common to both cell lines, there were distinctive patterns in the lipidomes. Thus, the lipidome of Caco2 cells was more heterogeneous and rich in cholesterol esters and triglycerides whilst HT29-MTX cells has a distinctive lipidome relating to phosphatidylethanolamines, phosphatidylinositols and odd chain lipids, including C17 fatty acids.

Conclusion: DESI-MSI has shown that Caco2 and HT29-MTX cells have distinctive lipidomes which are still evident when the cells are cocultured. It has potential to both allow further validation of these widely used cell models and provide insights into how dietary components may modify lipid metabolism in future.

1. Introduction

Cell-based models of the intestinal epithelium are often used to study intestinal transport of dietary molecules – from micronutrients such as iron, to toxicants and allergens [1-3]. The mainstay of these models is the Caco2 cell line which was derived from a human colorectal adenocarcinoma in 1977 and has since become the most widely used and best characterised intestinal cell line. It has the ability to mimic the morphological and functional characteristics to gut enterocytes by forming tight junctions between the cells and differentiating to form a brush border with microvilli on the apical surface of the cell [1]. An important metabolic activity of the enterocytes is the uptake of free fatty acids from the apical side, their re-synthesis into triglycerides which are then secreted on the basolateral side to be transported in the lymphatic system. Caco2 cell models demonstrate this behaviour and have been used to study lipid uptake and transport over many years [4-10] but have several limitations as, even when differentiated, they retain much of the character of cancer cell lines [11]. They cannot mimic the combination of different cell types found in the intestinal epithelium, such as goblet cells (mucus producing cells), endocrine cells, and M cells and consequently lack a mucus layer. One option for improving the cellular models is to use effective co-culture systems, one of which employs HT29-MTX cells which can act as model of goblet cells [12] and has been optimised regarding factors such as seeding ratios of Caco2 and HT29-MTX cells [13]. In addition to providing a mucus layer, co-culturing Caco2 and HT29-MTX cells has also been shown to rescue the epithelial phenotypes of the Caco2 cells more effectively, an effect that is further enhanced through interactions mediated by oleic acid [11]. However, the wider impact of co-culturing these cell types on lipid metabolism has not been directly investigated.

A highly effective technique for mapping lipids in biological samples is mass spectrometry imaging (MSI), the abundance and high ionisation efficiency of lipids enabling detection of many different lipid species based on their mass:charge ratios. It can be undertaken without the need for deuterated lipid standards [14]. Consequently MSI has been used to provide insights into the spatial distribution of lipids in various types of cells and tissues, supporting, for example, improved diagnosis of diseases such as cancer [14, 15] and has previously been applied to study different lipid species and its special arrangement on the cell culture [14, 16]. Desorption electrospray ionisation (DESI) MSI overpasses many of the limitations of other MSI methods; for instance, its ability to ionise lipids under ambient conditions means minimal sample preparation is required and does not require a matrix to extract the analytes from a sample surface [17]. In addition, the ionisation of the analyte using DESI

method takes place outside the vacuum system to avoid possible delay in the analysis time and to prevent contamination of the target analytes [18]. Therefore, DESI-MS imaging has been used to discover to identify the most abundant lipid species found in Caco2 and HT29-MTX cells and investigate whether co-culturing modified the lipid composition of the in individual cell types.

2. Material and methods

2.1 Culture reagents

Caco2 and HT29-MTX cell lines were purchased from the American Type Culture Collection ATCC (Teddington London, UK). HTB-37™. Dulbecco's Modified Eagle Medium (DMEM) without L-glutamine, Dulbecco's Phosphate-Buffered Saline (DPBS), Foetal bovine serum albumin (BSA) and trypan blue solution (0.4 % (w/v)) were purchased from Sigma-Aldrich (Dorset, UK). Hank's Balanced Salt Solution (HBSS) and live/dead staining kit were purchased from ThermoFisher Scientific (Hertfordshire, UK) while penicillin/streptomycin and L-glutamine were from Invitrogen (Shropshire, UK). C-Chip disposable Haemocytometer was purchased from Labtech International Ltd (Heathfield, UK). The borosilicate glass coverslips with thickness no. 1.5 and 25 mm Ø (cat No.631-0172) were purchased from VWR (Leicestershire, UK). Cell culture plasticware was purchased either from Cellstar, Greiner Bio-One (Stonehouse, UK). All other reagents (at least of analytical reagent grade) and plasticware were purchased from Sigma-Aldrich (Dorset, UK).

2.2 Sample preparation

Caco2 and HT29-MTX cells were cultured separately in bulk in 25 cm^2 flasks at 37 ºC, 5% CO_2 for 2-3 days. DMEM complete media supplemented with 20% (v/v) foetal serum bovine, 1% (w/v) non-essential amino acids, 1% (w/v) L-glutamine and 1% (w/v) penicillin-streptomycin was used as culture medium. On reaching 80–90% confluency cells were trypsinised and then seeded on a coverslip at a density of $1x10^5$ cells/ml either as separate cultures or in a co-culture system seeded at ratios of 75:25, 50:50 and 25:75 (Caco2: HT29-MTXcells). After seeding, each coverslip was placed in the well of a 6-well cell culture plate, and incubated at 37 ºC, 5% CO_2. Media was changed every 48 h for 21 days until cells were confluent. Cells were prepared for DESI MSI analysis by rinsing coverslips in 150 mM ammonium acetate, pH 7.1 for 30 s before being allowed to dry in the air stream of a biological safety cabinet for 15 min. Coverslips were then thoroughly dried using a vacuum desiccator for 15 min before storage at -80 °C in petri dishes until required.

2.3 Cell Viability Staining

Staining was performed according to the kit instructions. Briefly the staining solution was prepared by adding 15 µl ethidium homodimer (EthD-1) and 5 µl calcein to 10 ml of DPBS. Cells were washed with pre-warmed DPBS

(3 x 5 min) to remove any residual medium before adding 300 µl of the stain solution and incubating for 30-40 min at ambient temperature. Cells were visualised and imaged using fluorescence microscope EVOS FL (Life technologies Ltd, Paisley, UK), using either a a standard fluorescein bandpass filter emission 494 nm (green) for calcein and filters for propidium iodide emission 535 nm (red) for EthD-1. The green (live cells) and red (dead cells) images were then merged using the fluorescence microscope This analysis demonstrated x% of live cells for each culture..

2.4 DESI MS imaging

Mass spectrometry imaging using 2D DESI source (Prosolia) was conducted at Waters Corporation (Wilmslow, UK). Dried cell cultures gown on coverslips were mounted on microscope glass slides using double sided tape. Slides were scanned using Epson perfection V600 photo scanner. Scanned images were imported and the area where cells were confluent was selected using the co-registered photographic image of the samples in High-Definition Imaging (HDI) 1.5. Imaging experiments were carried out on a DESI (Prosolia, USA) mounted on a Xevo-G2-XS quadrupole-time of flight (QTOF) mass spectrometer (Waters Corporation, Wilmslow, UK). The DESI spray was composed of a solvent mixture of 98:2% MeOH: water (v/v) delivered at a flow rate of 2 µl/min with nebulizing gas pressure of 5 bar. The sprayer geometric positions were set that the sprayer was 1.5 mm above sample surface and the distance between sprayer to capillary was 6mm. The source temperature was 100 °C. For both positive and negative ionization modes, the acquisition mass range was 50-1200 m/z. DESI MSI experiments were performed using the scan rate of 2 scan/ second in positive mode and 4 scan/ second in negative mode. The X and Y pixel sizes were set at 20 µm.

2.5 DESI MS/MS

Selected precursor ions in both positive and negative ionisation modes (including m/z 810.55 and m/z 773.53) were further analysed using MS/MS. The experiments were carried out on a DESI (Prosolia, place, USA) mounted on a Xevo-G2-XS Q-TOF mass spectrometer (Waters Corporation, Wilmslow, UK). Spray conditions were the same as DESI imaging. Spectra were visualised using MassLynx (Waters Corporation, Wilmslow, UK).

2.6 MS data analysis

Raw data from each biological condition were processed using HDI software version 1.5 (Waters Corporation, Wilmslow, UK) to provide ion images from a consolidated list of m/z common to the different datasets as well as the unique m/z. Ion images were normalised to total ion current (TIC). Regions of interest (ROIs) were drawn directly from the DESI images that produced a .csv file containing average TIC normalised intensities which

was used for statistical analysis using MetaboAnalyst1 (https://www.metaboanalyst.ca/MetaboAnalyst/faces/home.xhtml) to compare between selected lipids that are presented in the two cell lines. Similarly, MSI analysis of Caco2/HT29-MTX co-culture was performed using the same criteria of DESI images with the same precursor ions mentioned above. For pixel classification of DESI imaging datasets, a Waters Corporation (WRC, Budapest, Hungary) prototype AMX MS imaging software was used in combination with HDI software.

3. Results

3.1 Fluorescence microscopy of cell cultures

Cultures with the model goblet cell line HT29-MTX showed clear evidence of the production of mucus with an amorphous fluorescent green staining mass evident (Fig. S1 b-d). A small number of red-staining dead cells were observed scattered across the coverslips interspersing the live cells, especially in the cultures containing the HT29-MTX cells but the presence of the mucus obscured the images preventing the enumeration of live/dead cells.

3.2 Lipid mapping of Caco2 and HT29-MTX cells

Initially the lipid composition of Caco2 and HT29-MTX cells was characterised by imaging using DESI MS in both positive and negative ionisation modes. Mass events relating to putative lipid species were selected and identified using a combination of accurate mass searching of the LipidMaps database and MS/MS analysis. Examples of combined spectra for a selected region of interest from MS images of Caco2 and HT29-MTX cells are shown in Fig. 1 and 2 respectively and the lipids identified in positive and negative ionisation modes are listed in Table 1. Na^+ and K^+ adducts were frequenty identified in the spectra, a common occurance as lipids have an affinity for sodium and potassium ions.

The positive ionization mode combined spectrum of the imaged Caco2 cells (Fig. 1a) was dominated by species ionising within the mass:charge range of 600-1000 m/z, certain of which could be annotated as lipids (Fig. 1b). The most intense peak of m/z 798.54 and a less intense species at m/z 770.51 corresponded to phosphatidyl cholines with long chain fatty acids (16:0_16:1 and 16:0_18:1 respectively). Other peaks of m/z 617.52 and 659.51 were identifed as cholesterol esters (CE, 14:1 and 16:1 respectively), a peak of m/z of 897.73 corresponding to a triglyceride (Fig. 1b, Table 1). Fewer species were observed in negative ionisation mode (Fig. 1d) and included putative lipid species at m/z 281 and 309.28 corresponding to oleic and eicosenoic acids. An ion of m/z 742.54 was putatively identified as a phosphatidylethanolamine (Table 1) whilst an ion of m/z 773.53 was identified as a phosphatidyglyceride PG 18:1/18:1 with the loss of a hydrogen ion using MS/MS

analysis (Supplementary Fig. S2). Fragmentation at m/z 491.28 resulted from the loss of ketene group which then facilitates the specific loss of the fatty acid chain of 18:1. A fragment was detected at m/z 417.25 which indicates the loss of the glycerol head group whilst another fragment detected at m/z 281.25 demonstrated the loss of fatty acid chain of 18:1.

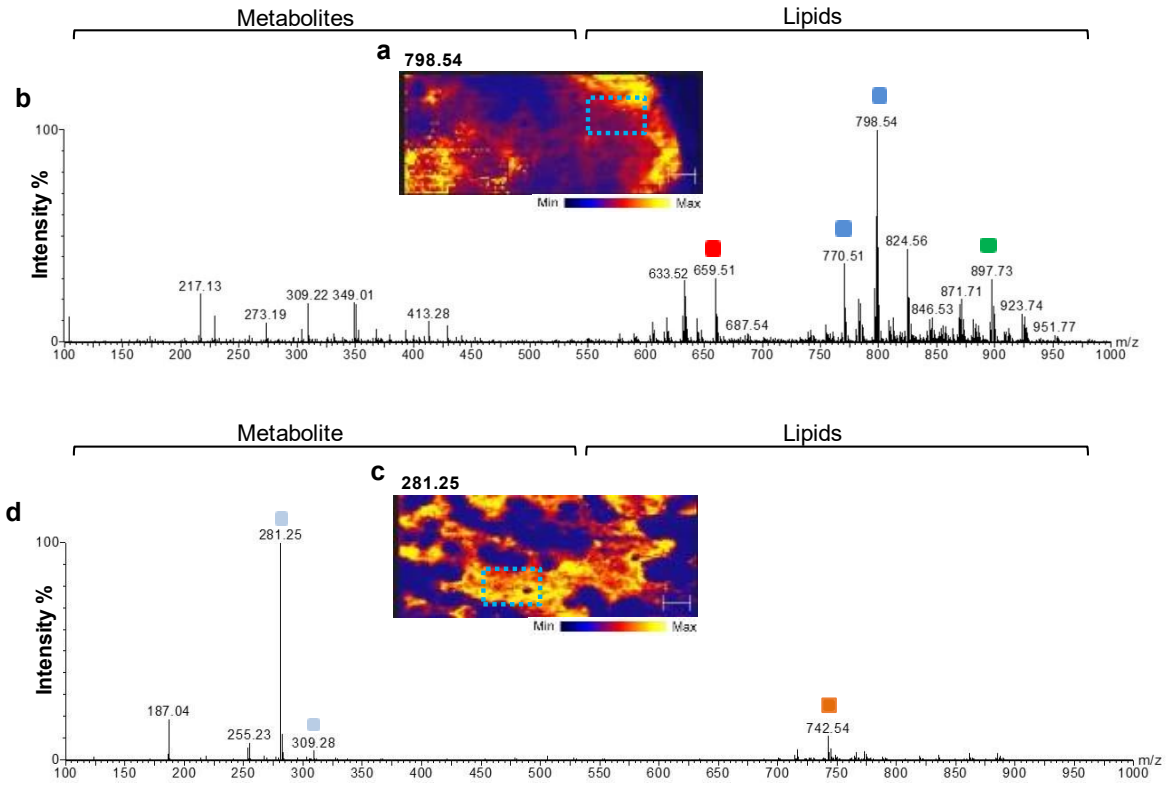

Fig. 1: Combined mass spectra of a region of interest from a MS image of Caco2 cells collected in positive (a, b) and negative (c, d) ionization modes. MS images of cells collected in positive (a) and negative (c) ionization modes coloured by intensity for lipid species. The pale blue dotted box represents the region of interest from which the combined spectra were derived for either positive (b) or negative (c) ionization modes. The lipid ions selected for DESI MS imaging are indicated as follows; positive ionization mode: ■ - cholesterol ester; ■ – phosphatidylcholine; and ■ - triglyceride. Negative ionization mode: ■ - fatty acids (oleic acid [m/z 281.25], and eicosenoic acid, [m/z 310.28], respectively) and ■ - phosphatidylethanolamine.

HT29-MTX cells gave a very similar combined positive ionisation mode mass spectrum to that of the Caco2 cells (Fig. 3c) with many of the same lipid species present. Three notable differences were observed. One of these was a lipid species with a m/z value of 756.53 which was only detected in the HT29-MTX cells and was identified as an unusual phosphatidyl choline with an odd chain fatty acid (PC31:1 K+). A second lipid with a m/z of 784.56 was identified as PC O34:1, which was present in both cell types but more abundant in the HT29-MTX cells. A third lipid species observed only in the HT29-MTX cells had a m/z of 810.55 which was identifed as being PC

(17:1_18:1) using MS/MS analysis (Supplementary Fig. S3). As the bonds attaching the phosphatidylcholine moiety are the weakest points in the molecule during the MS/MS fragmentation, the PC shows a neutral loss of the choline head group $N(CH_3)_3$ generating a fragment of m/z 751.47. The fragmentation also demonstrates mainly the loss of fatty acid chains (17:1 and 18:1) at m/z 558.74 and 537.48. A similar mass shift was detected as a result of the loss of potassium (K+) associated with fragment m/z 589.53. Other lipid ions at m/z 672.50, 700.53, 722.51, and 863.57 were only seen in negative ionization mode of HT29-MTX spectrum (Fig.3c) and corresponded to phosphatidylethanolamine (PE) and phosphatidylinositol (PI) respectively.

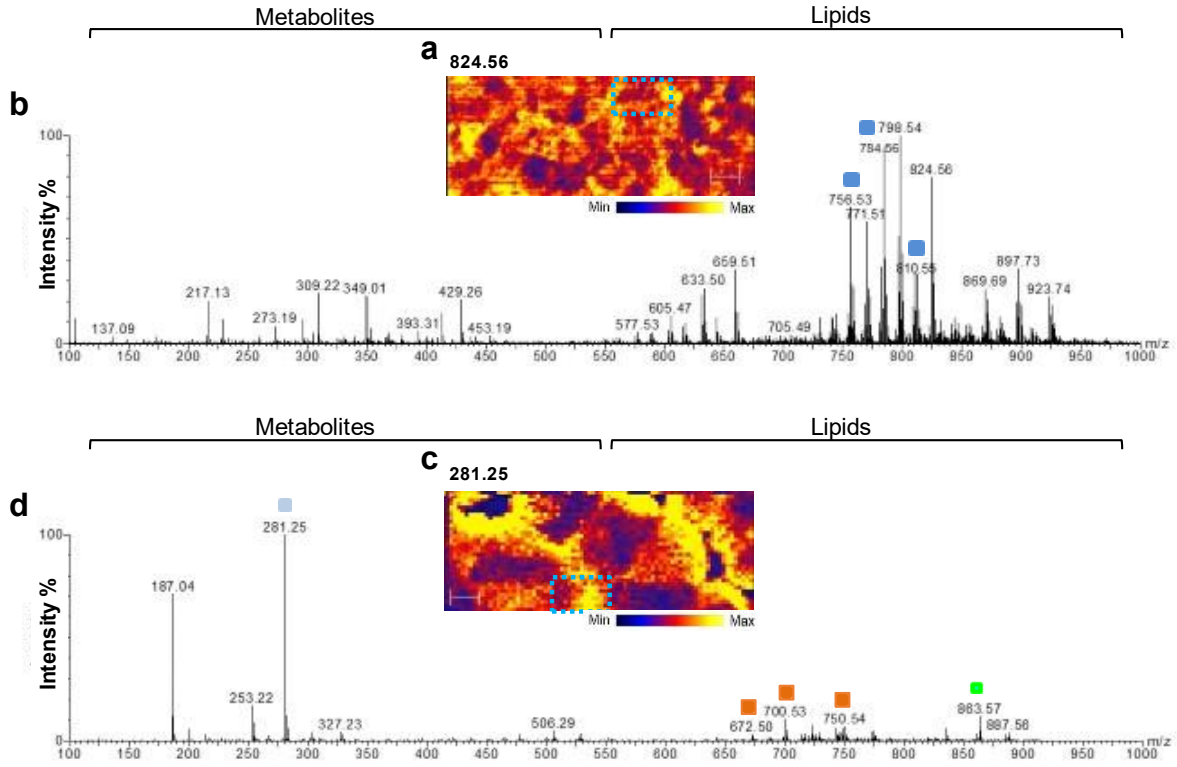

Fig. 2: Combined mass spectra of as region of interest from a MS image of HT29-MTX cells collected in positive (a, b) and negative (c, d) ionization modes. MS images of cells collected in positive (a) and negative (c) ionization modes coloured by intensity for lipid species. The pale blue dotted box represents the region of interest from which the combined spectra were derived for either positive (b) or negative (c) ionization modes. The lipid ions selected for DESI MS imaging comparison are indicated as follows; positive ionization mode: ■ – phosphatidylcholine. Negative ionization mode: ■ - phosphatidylethanolamine and phosphatidylinositol.

DESI imaging analysis in both positive and negative ionisation mode was then combined with principal component analysis (PCA) to establish similarities and differences in lipid species between the Caco2 and HT29-MTX cell types (Figs. 3a and 4a). They could be clearly separated based on principle component 1 which

accounted for 78.2% of variation, whist PC2 represented variance in the different types of lipid species identified (Supplementary Fig. S4). Interestingly, imaging in both positive and negative ionisation modes showed greater variation between ROI for the Caco2 cells compared to the HT-29MTX cells, particularly with regards PC2. This may relate to greater heterogeneity in the lipid species found in the Caco2 cells, perhaps reflecting minor variations in the way in which individual cells differentiate after reaching confluence.

Lipid species contributing to separation of Caco2 and HT29-MTX cells on PCA were selected and used to generate DESI MS images specific for particular lipid species (Figs. 3b, c and 4 b, c). This showed that the Caco2 cells contained higher levels of the cholesterol esters (14:1 and 16:1), phosphatidyl choline (16:0_16:1), together with a triglyceride (55:5), oleic [(18:1) at m/z 281.25] and eicosenoic [20:1; m/z 309.28] acids, the latter having a distinctive distribution compared to oleic acid which was more uniformly found. In contrast the HT-29MTX cells were enriched in several types of phosphatidyl choline including PC31-1 and PC17_1_18_1. They were also enriched in two ether lipids, PC (O-32-1), m/z 740.55 (corresponding to either 14:0_18:1 or 16:0_16:1) and PC (O-34-1), m/z 784.56 (corresponding to either 16:0_18:1or 18:0_16:1). It is clear from the images that PC31-1 and PC (O-32-1) were present in clusters of cells, whereas PC (O-34-1) and PC17:1_18:1 were distributed more homogeneously across the culture.

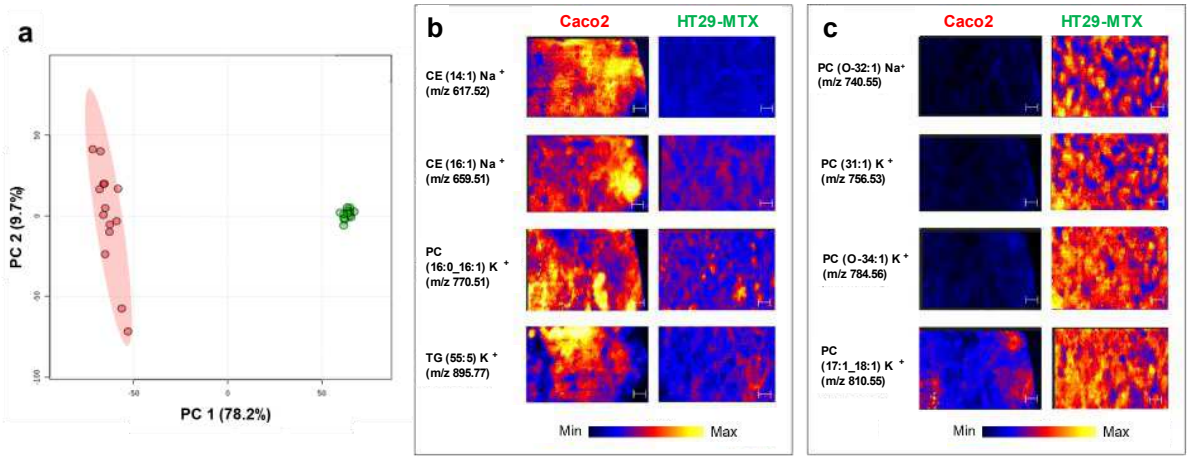

Fig. 3: Comparison of the spatial distribution of lipids in Caco2 and HT29-MTX cell cultures imaged using DESI in positive ionisation mode. (a) Thirteen regions of interest (RoI) of 0.50 mm^2 were selected from each MS image and principal component analysis (PCA) used to identify lipids that were differentially expressed between the two cell lines. ROIs from Caco2 cells are shown by the red circles and HT29-MTX cells by green circles. Loadings from PCA plots (Supplementary information Figure S4) were used to identify lipids

predominantly found in either Caco2 cells (b) or HT29-MTX cells (c). The scale bar=1.48 mm. The intensity of the lipid molecule was in a range of 0-0.025 (min-max). Lipid identifications are summarized in Table 1.

DESI imaging in negative ionisation mode also showed the cell types were differentially enriched with various types of phosphatidyl ethanolamines (PE) (Fig. 4b, c). Thus, Caco2 cells contained higher levels of PE 36:1 and 36:2 whilst the HT29-MTX cells were enriched in PE's appearing as multiply charged molecules. These included a PE-32:1 of m/z 672.50, which was the second-highest relative intensity lipid identified using negative ionisation mode which was nevertheless heterogeneously distributed across the culture. This was accompanied by two ether PE's of m/z 700.53 (O-34.2) and 722.51 (O-36:5), the former being present at a low level in only certain areas of the culture, whilst the latter was homogeneously distributed across the culture. Interestingly phosphatidylinositol (PI36-1, m/z 863.57) was also observed only in HT29-MTX cell culture and showed a very heterogenous distribution.

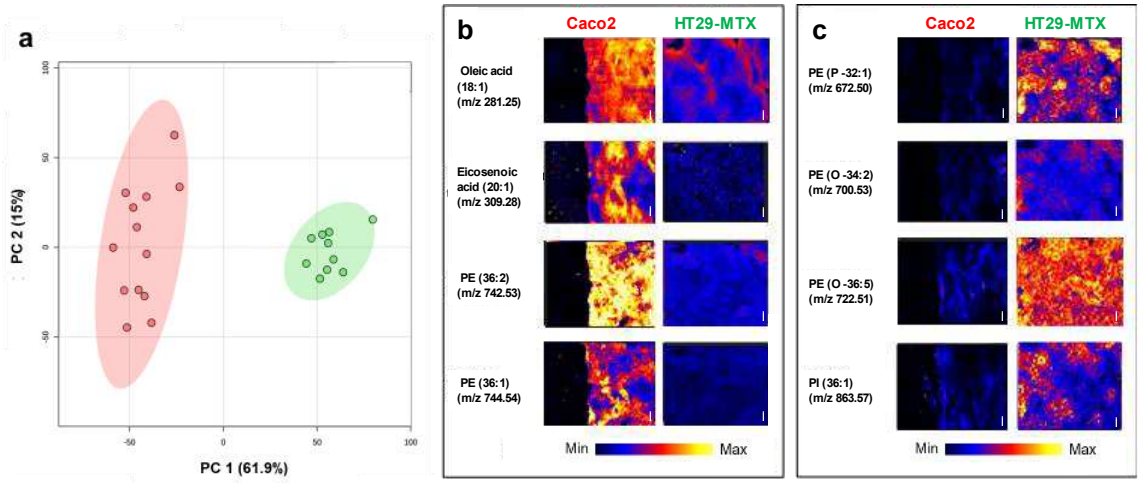

Fig. 4: Comparison of the spatial distribution of lipids in Caco2 and HT29-MTX cell cultures imaged in negative ionisation mode. (a) Thirteen regions of interest (RoI indicated by circles) of 0.50 mm^2 were selected from each MS image and principal component analysis (PCA) used to identify lipids that were differentially expressed between the two cell lines. Red circles - Caco2 cell culture; green circles - HT29-MTX cultures. Loadings from PCA plots (Supplementary Figure S4) were used to identify lipids predominantly found in either Caco2 cells (b) or HT29-MTX cells (c). The scale bar=1.48 mm. The intensity of the lipid molecule was in a range of 0-0.025 (min-max). Lipid identifications are summarized in Table 1.

3.3 Effect of co-culturing Caco2 and HT-29 MTX cells on lipid compostion

DESI imaging of the individual cell types and co-cultures seeded using different ratios of Caco2:HT29-MTX cells was then undertaken and lipid features able to discriminate between the different cell cultures identified using PCA analysis (Figs. 5A and 6A). The data acquired in positive ionization mode showed that whilst PCs (31:1), (O-34:1), and (17:1_18:1) were largely absent from the Caco2 cells when singly cultured, they started to appear at a low level in the co-culture system, the abundance increasing as the seeding ratio of HT29-MTX cells increased (Fig. 5b). In contrast, TG

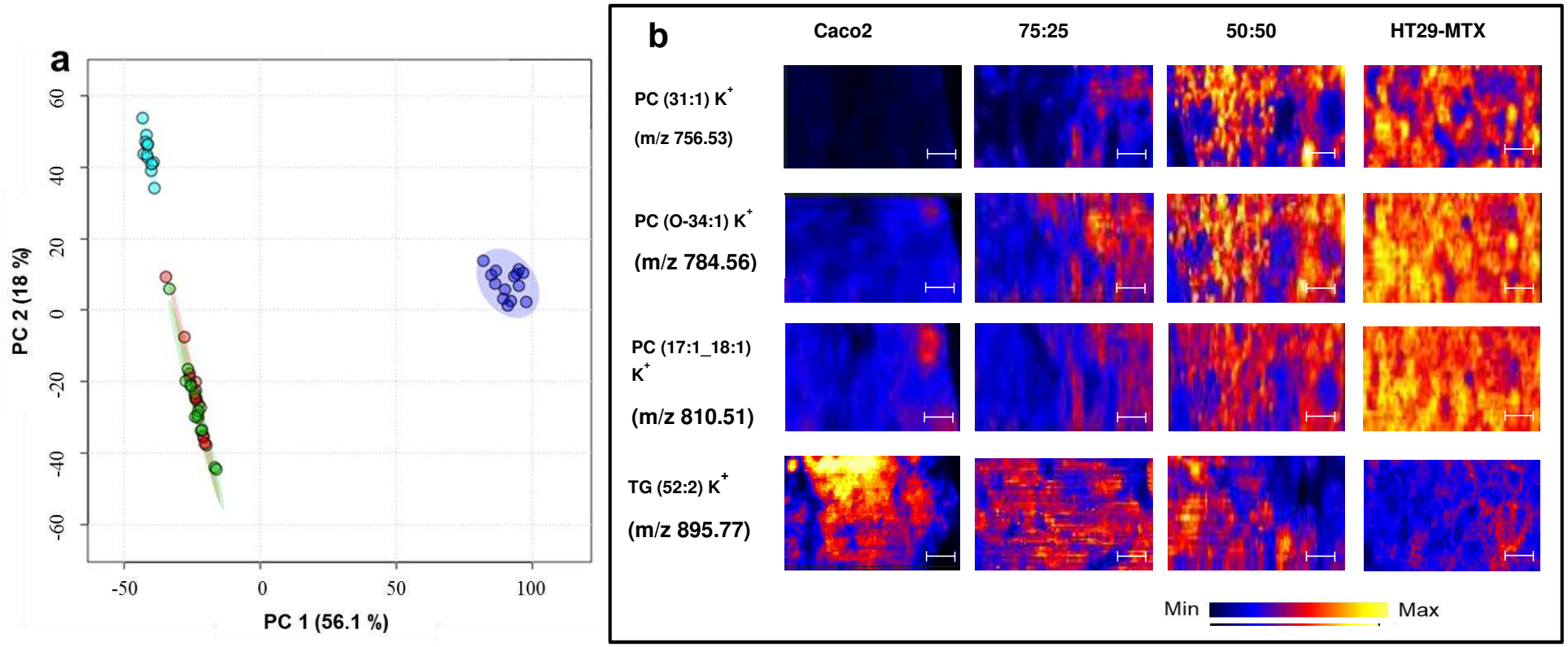

Fig. 5: Comparison of the spatial distribution of lipids in co-cultures of Caco2 and HT29-MTX cells imaged in positive ionisation mode. (a) Principal components analysis of thirteen ROIs, 0.50 mm^2 for each MS image, each dot representing one region of interest coloured as follows: purple - Caco2 cells; turquoise - HT29-MTX cells; green - co-culture seeded with a ratio of Caco2-HT-29MTX cells of 75:25; red - dots co-culture seeded with a ratio of Caco2-HT-29MTX cells of 50:50. Loadings (Supplementary information Figure S5) were used to identify lipids responsible for the clustering of the ROIs; the distribution of these was then visualized across the images (b). The scale bar=1.48 mm. The intensity of the lipid molecule was in a range of 0-0.025 (min-max). Lipid identifications are summarized in Table 1.

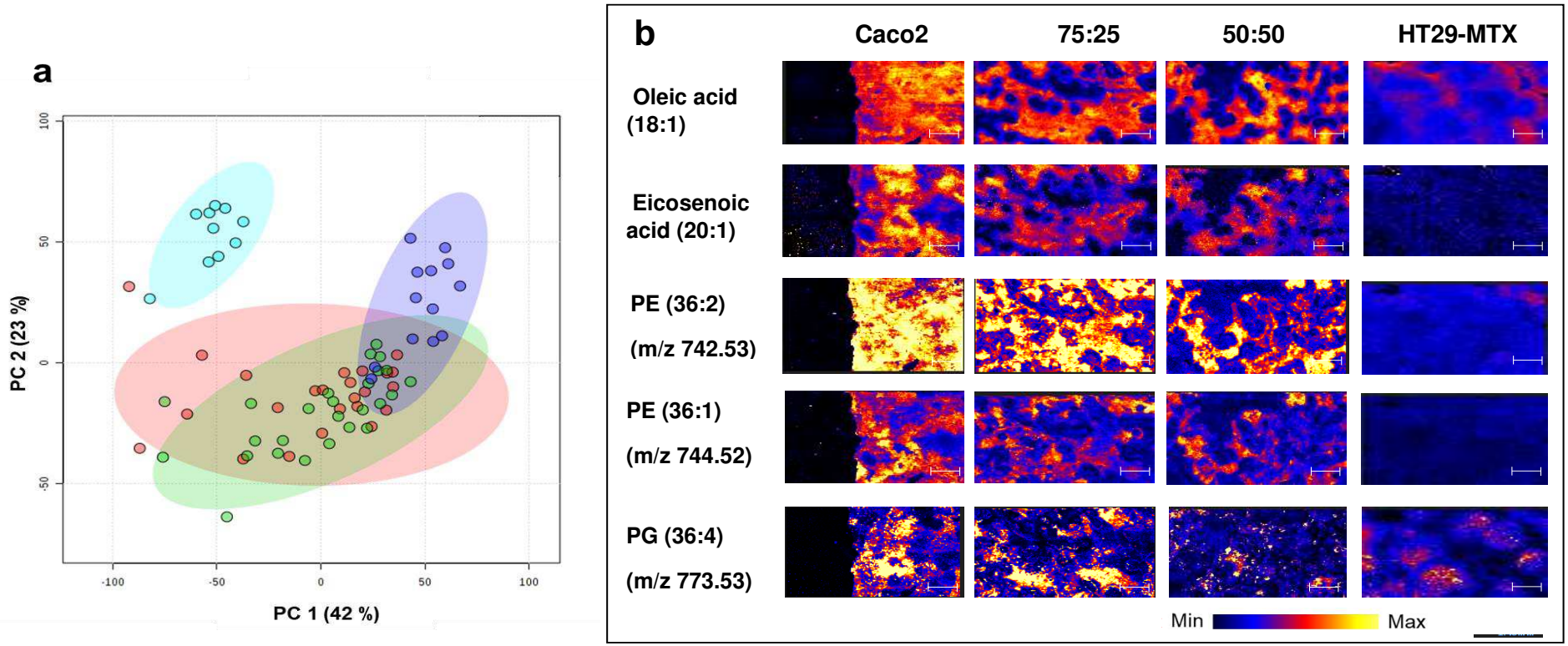

Fig. 6: Comparison of the spatial distribution of lipids in cocultures Caco2 and HT29-MTX cell imaged in negative ionisation mode. (a) Principal components analysis of thirteen ROIs, each 0.50 mm^2. Each dot represents one region of interest each ROI and are coloured as follows: purple - Caco2 cells; turquoise - HT29-MTX cells; green - co-culture seeded with a ratio of Caco2-HT-29MTX cells of 75:25; red - dots co-culture seeded with a ratio of Caco2-HT-29MTX cells of 50:50. Loadings (Supplementary information Figure S5) were used to identify lipids responsible for the clustering and visualized across the images (b). The scale bar=1.48 mm. The intensity of the lipid molecule was in a range of 0-0.025 (min-max). Lipid identifications are summarized in Table 1.

(52:2) was more abundant in the singly cultured Caco2 cells and the 75:25 co-culture but was reduced in the 50:50 co-culture and was of very low abundance in the singly cultured HT29-MTX cells.

Imaging under negative ionisation mode showed that when the seeding density of Caco2 cells was decreased, the distribution of oleic (18:1) and eicosenoic acid (20:1) together with PEs (including long chains PEs (36:2 [either as 16:0_20:2, 18:0_18:2, or 18:1_18:1] and 36:1) were decreased, suggesting that these lipids orignated from the Caco2 cell cultures (Fig. 6 a). Phosphatidylglycerol (PG) (36:4; either 16:0_20:2, 18:0_18:2, or 18:1_18:1) was found to be more abundant in singly cultured Caco2 cells and the 75:25 co-culture and had a heterogeneous distribution (Fig. 6b).

Further data analysis was performed to be able to distinguish in the co-culture cell samples where Caco2 and HT29.MTX cells were localised. A workflow was developed which consisted of building and validating a PCA and linear discriminant analysis (LDA) statistical model using the protype AMX Imaging software using DESI imaging datasets for the singly cultured Cacao2 and HT29-MTX cells (Supplementary Fig. S5). When the model was applied to the 25:75, 50:50, and 75:25 co-culture DESI imaging datasets, for both positive and negative mode, it allowed the different cell types to be identified in the DESI images (Fig. 7). The ratio of pixels classified Caco2/HT29-MTX is correlated with the ratio of the cell lines used for seeding of the co-culture and showed the heterogeneous way in which the co-cultures grow. Thus, although the 25:75 seeding ratio of HT29-MTX: Caco2 cells resulted in a distribution of the HT29-MTX cells within the Caco2 cells, this distribution was not achieved when seeding using a ratio of 75:25. This might reflect the difficulty of resuspending the Caco2 cells in the HT29-MTX cells because of the mucus that they produce.

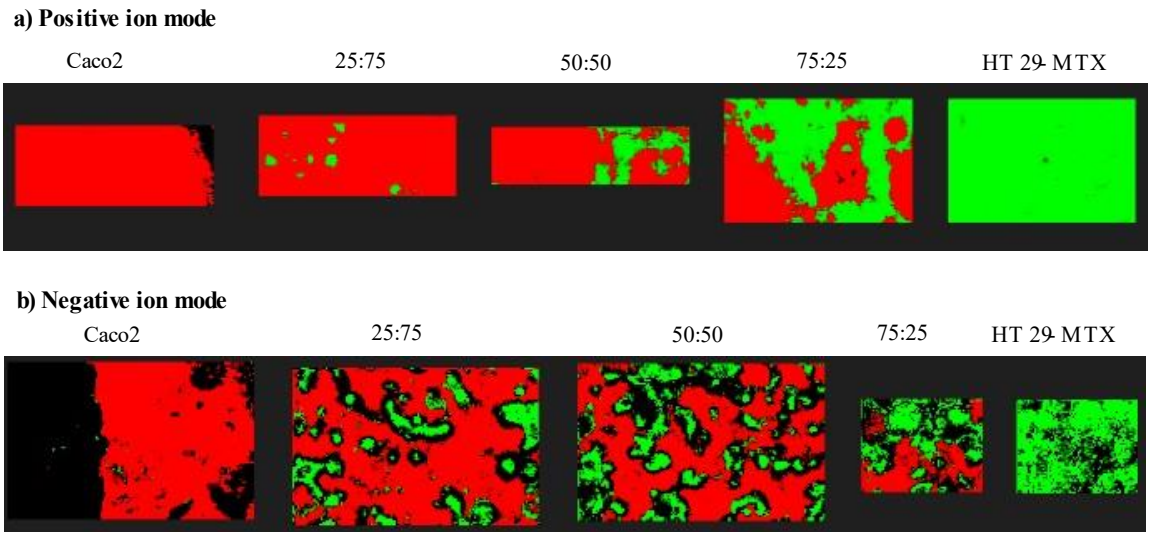

Fig. 7: Mass spectrometry imaging of Caco2 and HT-29MTX cells within co-cultures.

Pixel classification images resulting from the application of the A statistical model was built based on DESI imaging datasets of either 100% Caco2 or 100% HT29-MTX cells. Pixels classified as Caco2 cells are coloured green, whilst pixels classified as HT29-MTX cells are coloured red. and black pixels were identified either as media or outliner**.**

4. Discussion

DESI-MIS has been applied for the first time to the anaysis of two important cell models of the gut epithelium which has allowed the spatial distribution of the distinct lipid species to be mapped.

The detection of CE (14:1 and 16:1), PCs (16:0_16:1) and TG (16:1_16:1_20:0) in both cell lines and their greater abundance in Caco2 cells is consistent with their known capacity to synthesise cholesterol and cholesterol esters, phosphatidyl cholines and triglycerides [6, 19]. The greater abundance of these lipids in Caco2 cells may reflect their being more enterocyte-like and hence have the capacity to absorb and re-synthesis lipids. HT-29MTX cells have been less characterised with regards their lipid composition and, being considered to be better model of goblet cells, are less actively involved in lipid uptake and re-synthesis of triglycerides. Both cells were abundant in PC, although the relative content of HT29-MTX cells may reflect their being a better model of mucus-producing Goblet cells. In addition to the widespread occurance of different PC lipid species in cell membranes, it has been founds that PCs accumulate on the gut epithelial surface where they have been found to associate with the mucus layer forming a hydrophobic barrier against any bacterial attack [20, 21] and is consistent with the greater abundance of PC's observed on the mucus-secreting HT29-MTX cells. Two

tyes of lipid species, PE and PI, could also be considered as biomarkers for HT29-MTX cell cultures as they were not found in the Caco2 cells.

In this study, some lipid species were observed as an odd number fatty acid chain such as; PC (31:1), and PC (17:1_18:1). This is an unusual phenomenon since most of the fatty acid chains are even chain number composed of carbon chain length of 2–26 in 99 % of the total plasma concentration in humans [22]. The odd-chain fatty acids, such as C15:0 have been associated with dietary intake of animal fat in rats, whilst C17:0 fatty acids appear to by produced as a consequence of endogenous metabolism through α-oxidation [23]. Recent studies reported that the odd-chain fatty acids in human tissue are an important biomarker for coronary heart disease (CHD) risk and type II diabetes mellitus (T2D) risk and are used as biomarkers for dietary food intake evaluation [24-26]. In this study, most of the lipids that presented an odd carbon number were PC, and these lipids were highly distributed in HT29- MTX. The odd chain fatty acids, such as pentadecanoic acid (15:0) and heptadecanoic acid (17:0), have been used as a marker of dairy fat intake as they arise from the use of propionate/butyrate in fatty acid synthesis in dairy cattle [25]. In general, these odd fatty chains are present only in trace amount in most animal tissues [27]. Although the C17 fatty acid could have originated from metabolism of dairy lipids arising from the use of bovine serum in the cell culture medium this seems unliely since the same culture medium was used for the Caco2 cells. Instead it seems more likely that it arises from an endogenous synthesis pathway which is only present in the HT29- MTX cells. Although odd-chain fatty acids can be generated through elongation of short chain fatty acids this seems an unlikely origin in cells cultured without a microbial source of short-cahin fatty acids [28]. Another source might be shortening of very long chains fatty acid (VLCFAs) through β-oxide of odd-chain VLCFAs resulting from 2-hydroxylated fatty acids as a consequence of peroxisomal α-oxidation [28].

The MSI also showed differential distribution of lipids across the cell cultures, with some lipids clustered in particular regions of the cell culture, the Caco2 cells generally showing much greater heterogenicty than the HT29-MTX cells. This is consistent with the greater heterogenity of Caco2 cells which may reflect the way in which theiy terminally differentiate upon reaching confluence. There is evidence from transcriptome analysis that the coculture system influences the repertoire of proteins expressed in Caco2 cells, with lipids playing an important role in mediating these changes [11]. Although this study indicates that the HT29-MTX lipid profile was clearly distinguishable, even in the co-culture system, furhter analysis would be reuqired to ascertain whether the Caco2 cell lipid metabolism is also altered in the presence of HT29-MTX cells.

5. Conclusion

DESI-MS imaging is a rapid, sensitive, and accurate technique that can be applied to the investigation of lipid heterogeneity on the cultures of numerous cells with minimal sample treatment. It provides insight into the inherent heterogenity of the cell cultures and has the potenital to act as a quality contorl tool for cell cultures. It is becoming evident that dietary lipids, suuch as oleic acid [11] and short-chain fatty acids originating from either metabolism of dietary componds or from the microbiota, maybe transformed by these different cell types [23]. Understanding how they might modify the lipidome of these intestinal cell models will be important as they are increasingly used in an elaborated form to investigate the impact of uptake on other cells types ranging from adipocytes to studying inflammation [29, 30].

Declarations

Funding

This research is conducted at the University of Manchester with funding from Al-Baha University in Saudi Arabia and an N8 Agri-Food Pump priming grant.

Ethical approval and consent to participate

Not applicable.

Consent for publication

All authors agreed with the content of the article and approved its submission for publication.

Conflict of interest

Emmanuelle Claude and Lee Gethings are employees of Waters Corporation the vendor of mass spectrometry equipment used in this study.

Availability of data and material

MS imaging data are available on request.

Author contribution statement

The work was initiated and concieved by CM; HM undertook the cell culture work and data analysis. EC supervised and undertook the MS imaging analysis. HM, EC and CM drafted the manuscript and LG reviewed the MS analysis and the manuscript.

Acknowledgements

We would like to thank Chiara Nitride, Charlotte hands and Matthew daly for helpful discussions and support.

References

1. Angelis ID, Turco L. Caco-2 cells as a model for intestinal absorption. Current protocols in toxicology. 2011;Chapter 20:Unit20.6. doi: 10.1002/0471140856.tx2006s47.

2. Glahn RP, Wortley GM, South PK, Miller DD. Inhibition of iron uptake by phytic acid, tannic acid, and ZnCl2: studies using an in vitro digestion/Caco-2 cell model. J Agric Food Chem. 2002;50(2):390-5.

3. Tran VN, Viktorová J, Ruml T. Mycotoxins: Biotransformation and Bioavailability Assessment Using Caco-2 Cell Monolayer. Toxins. 2020;12(10). doi: 10.3390/toxins12100628.

4. Shamir R, Johnson WJ, Zolfaghari R, Lee HS, Fisher EA. Role of bile salt-dependent cholesteryl ester hydrolase in the uptake of micellar cholesterol by intestinal cells. Biochemistry. 1995;34(19):6351-8. doi: 10.1021/bi00019a013.

5. Srivastava RA, Ito H, Hess M, Srivastava N, Schonfeld G. Regulation of low density lipoprotein receptor gene expression in HepG2 and Caco2 cells by palmitate, oleate, and 25-hydroxycholesterol. Journal of lipid research. 1995;36(7):1434-46.

6. Mehran M, Levy E, Bendayan M, Seidman E. Lipid, apolipoprotein, and lipoprotein synthesis and secretion during cellular differentiation in Caco-2 cells. In vitro cellular & developmental biology Animal. 1997;33(2):118-28.

7. Schneider AC, Mignolet E, Schneider YJ, Larondelle Y. Uptake of conjugated linolenic acids and conversion to cis-9, trans-11-or trans-9, trans-11-conjugated linoleic acids in Caco-2 cells. Br J Nutr. 2013;109(1):57-64. doi: 10.1017/s0007114512000608.

8. Yang F, Chen G, Ma M, Qiu N, Zhu L, Li J. Fatty acids modulate the expression levels of key proteins for cholesterol absorption in Caco-2 monolayer. Lipids in health and disease. 2018;17(1):32. doi: 10.1186/s12944-018-0675-y.

9. van Greevenbroek MM, Voorhout WF, Erkelens DW, van Meer G, de Bruin TW. Palmitic acid and linoleic acid metabolism in Caco-2 cells: different triglyceride synthesis and lipoprotein secretion. Journal of lipid research. 1995;36(1):13-24.

10. Werno MW, Wilhelmi I, Kuropka B, Ebert F, Freund C, Schurmann A. The GTPase ARFRP1 affects lipid droplet protein composition and triglyceride release from intracellular storage of

intestinal Caco-2 cells. Biochem Biophys Res Commun. 2018;506(1):259-65. doi: 10.1016/j.bbrc.2018.10.092.

11. Berger E, Nassra M, Atgié C, Plaisancié P, Géloën A. Oleic Acid Uptake Reveals the Rescued Enterocyte Phenotype of Colon Cancer Caco-2 by HT29-MTX Cells in Co-Culture Mode. Int J Mol Sci. 2017;18(7). doi: 10.3390/ijms18071573.

12. Wikman-Larhed A, Artursson P. Co-cultures of human intestinal goblet (HT29-H) and absorptive (Caco-2) cells for studies of drug and peptide absorption. European Journal of Pharmaceutical Sciences. 1995;3(3):171-83. doi: https://doi.org/10.1016/0928-0987(95)00007-Z.

13. Lozoya-Agullo I, Araújo F, González-Álvarez I, Merino-Sanjuán M, González-Álvarez M, Bermejo M, et al. Usefulness of Caco-2/HT29-MTX and Caco-2/HT29-MTX/Raji B Coculture Models To Predict Intestinal and Colonic Permeability Compared to Caco-2 Monoculture. Molecular pharmaceutics. 2017;14(4):1264-70. doi: 10.1021/acs.molpharmaceut.6b01165.

14. Bowman AP, Heeren RMA, Ellis SR. Advances in mass spectrometry imaging enabling observation of localised lipid biochemistry within tissues. TrAC Trends in Analytical Chemistry. 2019;120:115197. doi: https://doi.org/10.1016/j.trac.2018.07.012.

15. Buchberger AR, DeLaney K, Johnson J, Li L. Mass Spectrometry Imaging: A Review of Emerging Advancements and Future Insights. Analytical chemistry. 2018;90(1):240-65. doi: 10.1021/acs.analchem.7b04733.

16. Berry KA, Hankin JA, Barkley RM, Spraggins JM, Caprioli RM, Murphy RC. MALDI imaging of lipid biochemistry in tissues by mass spectrometry. Chemical reviews. 2011;111(10):6491-512. doi: 10.1021/cr200280p.

17. Eberlin LS, Ferreira CR, Dill AL, Ifa DR, Cooks RG. Desorption electrospray ionization mass spectrometry for lipid characterization and biological tissue imaging. Biochimica et biophysica acta. 2011;1811(11):946-60. doi: 10.1016/j.bbalip.2011.05.006.

18. Manicke NE, Wiseman JM, Ifa DR, Cooks RG. Desorption electrospray ionization (DESI) mass spectrometry and tandem mass spectrometry (MS/MS) of phospholipids and sphingolipids: ionization, adduct formation, and fragmentation. Journal of the American Society for Mass Spectrometry. 2008;19(4):531-43. doi: 10.1016/j.jasms.2007.12.003.

19. Cerda SR, Wilkinson Jt, Broitman SA. Regulation of cholesterol synthesis in four colonic adenocarcinoma cell lines. Lipids. 1995;30(12):1083-92. doi: 10.1007/bf02536608.
20. Korytowski A, Abuillan W, Amadei F, Makky A, Gumiero A, Sinning I, et al. Accumulation of phosphatidylcholine on gut mucosal surface is not dominated by electrostatic interactions. Biochimica et biophysica acta Biomembranes. 2017;1859(5):959-65. doi: 10.1016/j.bbamem.2017.02.008.
21. Ehehalt R, Wagenblast J, Erben G, Lehmann WD, Hinz U, Merle U, et al. Phosphatidylcholine and lysophosphatidylcholine in intestinal mucus of ulcerative colitis patients. A quantitative approach by nanoElectrospray-tandem mass spectrometry. Scandinavian journal of gastroenterology. 2004;39(8):737-42. doi: 10.1080/00365520410006233.
22. Khaw KT, Friesen MD, Riboli E, Luben R, Wareham N. Plasma phospholipid fatty acid concentration and incident coronary heart disease in men and women: the EPIC-Norfolk prospective study. PLoS medicine. 2012;9(7):e1001255. doi: 10.1371/journal.pmed.1001255.
23. Jenkins BJ, Seyssel K, Chiu S, Pan PH, Lin SY, Stanley E, et al. Odd Chain Fatty Acids; New Insights of the Relationship Between the Gut Microbiota, Dietary Intake, Biosynthesis and Glucose Intolerance. Scientific reports. 2017;7:44845. doi: 10.1038/srep44845.
24. Kurotani K, Karunapema P, Jayaratne K, Sato M, Hayashi T, Kajio H, et al. Circulating odd-chain saturated fatty acids were associated with arteriosclerosis among patients with diabetes, dyslipidemia, or hypertension in Sri Lanka but not Japan. Nutrition research (New York, NY). 2018;50:82-93. doi: 10.1016/j.nutres.2017.12.004.
25. Venäläinen TM, Lankinen MA, Schwab US. Odd-chain fatty acids as dietary biomarkers for fiber and fish intake. Am J Clin Nutr. 2017;106(3):954. doi: 10.3945/ajcn.117.162347.
26. Matthan NR, Ooi EM, Van Horn L, Neuhouser ML, Woodman R, Lichtenstein AH. Plasma phospholipid fatty acid biomarkers of dietary fat quality and endogenous metabolism predict coronary heart disease risk: a nested case-control study within the Women's Health Initiative observational study. Journal of the American Heart Association. 2014;3(4). doi: 10.1161/jaha.113.000764.
27. Smedman AE, Gustafsson IB, Berglund LG, Vessby BO. Pentadecanoic acid in serum as a marker for intake of milk fat: relations between intake of milk fat and metabolic risk factors. Am J Clin Nutr. 1999;69(1):22-9. doi: 10.1093/ajcn/69.1.22.

28. Pfeuffer M, Jaudszus A. Pentadecanoic and Heptadecanoic Acids: Multifaceted Odd-Chain Fatty Acids. Advances in nutrition (Bethesda, Md). 2016;7(4):730-4. doi: 10.3945/an.115.011387.

29. Berger E, Géloën A. Adipocytes as lipid sensors of oleic acid transport through a functional Caco-2/HT29-MTX intestinal barrier. Adipocyte. 2019;8(1):83-97. doi: 10.1080/21623945.2019.1580842.

30. Ponce de León-Rodríguez MDC, Guyot JP, Laurent-Babot C. Intestinal in vitro cell culture models and their potential to study the effect of food components on intestinal inflammation. Crit Rev Food Sci Nutr. 2019;59(22):3648-66. doi: 10.1080/10408398.2018.1506734.

Table 1. Summary of all lipid species presented in the averaged spectrum Figure 1 and 2. These lipid species were identified by accurate mass searching from the LipidMaps database (www.lipidmaps.org) in Caco2, HT29-MTX cell cultures and co-culture system in positive and negative ionization mode. N/A- Not available. Dark grey shading indicates which cell culture type the putative lipid species was identified

Lipid	Experimental m/z	Theoretical m/z	MS/MS	Cultures			
				Caco2	75:25 Caco2:HT29-MTX	50:50 Caco2:HT29-MTX	HT29-MTX
Positive ionisation mode							
CE (14:1)	617.52	617.52	N/A	Yes	Yes		
CE (14:1) K^+	633.49	633.50	N/A	Yes	Yes	Yes	Yes
CE (16:1)	659.51	659.51	N/A	Yes			
PC (31:1) K^+	756.53	756.55	Yes				Yes
PC (16:0_ 16:1) K^+	770.51	770.50	Yes	Yes	Yes	Yes	Yes
PC (O-34:1) or PC (O-34:1) K^+ or PC (P-34:1) K^+	784.54	784.48	Yes			Yes	Yes
PC (16:0; 18:1) K^+	798.54	798.54	Yes	Yes	Yes	Yes	Yes
PC (17:1_ 18:1)	810.51	810.52	Yes				Yes
PC (36:2) K^+	824.55	824.54	N/A	Yes	Yes	Yes	Yes

Lipid	Experimental m/z	Theoretical m/z	MS/MS	Cultures			
				Caco2	75:25 Caco2:HT29-MTX	50:50 Caco2:HT29-MTX	HT29-MTX
TG (48:1) K^+	843.68	843.67	N/A				Yes
TG (50:1) K^+	871.71	871.71	N/A	Yes			
TG (52:1) Na^+	883.73	883.77	N/A	Yes	Yes	Yes	Yes
TG (16:1_16:1_20:0) K^+	897.72	897.72	N/A	Yes	Yes	Yes	Yes
TG (54:3) K^+	923.74	923.74	N/A	Yes	Yes	Yes	Yes
Negative ionisation mode							
FA (12:6)	187.04	187.07	N/A	Yes	Yes	Yes	Yes
FA (16:0)	255.23	255.23	N/A	Yes	Yes	Yes	Yes
FA (18:1)	281.25	281.24	N/A	Yes	Yes	Yes	Yes
FA (22:6)	327.23	327.23	N/A				Yes
FA (20:1)	309.28	309.27	N/A	Yes	Yes	Yes	Yes
LPC (17:1)	508.29	508.32	N/A				Yes
PE (P-32:1)	672.50	672.49	N/A				Yes
PE (O-34:2)	700.53	700.52	N/A				Yes
PE (36:2)	742.54	742.53	N/A	Yes			
PE (O-38:5)	750.54	750.54	N/A				Yes
PI (36:1)	863.56	863.56	N/A				Yes

Lipid	Experimental m/z	Theoretical m/z	MS/MS	Cultures			
				Caco2	75:25 Caco2:HT29-MTX	50:50 Caco2:HT29-MTX	HT29-MTX
PI (O-36:0)	887.56	887.57	N/A				Yes

Supplementary Files

This is a list of supplementary files associated with this preprint. Click to download.

- SupplInformationforMSIpaperver5.pdf